Suspended particle capture by synthetic vegetation in a laboratory flume

Article *in* Water Resources Research · October 2015

DOI: 10.1002/2014WR016481

CITATIONS
0

READS
23

4 authors, including:

Kristen Fauria
University of California, Berkeley
7 PUBLICATIONS **11** CITATIONS

SEE PROFILE

S. Geoffrey Schladow
University of California, Davis
139 PUBLICATIONS **2,838** CITATIONS

SEE PROFILE

AGU PUBLICATIONS

Water Resources Research

RESEARCH ARTICLE
10.1002/2014WR016481

Suspended particle capture by synthetic vegetation in a laboratory flume

Kristen E. Fauria[1,2,3], Rachel E. Kerwin[4,5], Daniel Nover[1,2,6], and S. Geoffrey Schladow[1,2]

[1]Department of Civil and Environmental Engineering, University of California, Davis, Davis, California, USA, [2]Tahoe Environmental Research Center, University of California, Davis, Incline Village, Nevada, USA, [3]Department of Earth and Planetary Science, University of California, Berkeley, Berkeley, California, USA, [4]Department of Plant Sciences, University of California, Davis, Davis, California, USA, [5]Department of Genetics, University of Georgia, Athens, Georgia, USA, [6]Center for Information Technology Research in the Interest of Society, School of Engineering, UC Merced, Merced, California, USA

Key Points:
- Synthetic plant-populated flumes remove more particles from suspension compared to bare flumes
- Presence of biofilm and low flow velocities increases capture rates and efficiencies
- Capture efficiency is a nonlinear function of stem density

Supporting Information:
- Supporting Information S1

Correspondence to:
K. E. Fauria,
kfauria@berkeley.edu

Citation:
Fauria, K. E., R. E. Kerwin, D. Nover, and S. Geoffrey Schladow (2015), Suspended particle capture by synthetic vegetation in a laboratory flume, *Water Resour. Res.*, *51*, doi:10.1002/2014WR016481.

Received 29 SEP 2014
Accepted 22 OCT 2015
Accepted article online 29 OCT 2015

Abstract Vegetated floodplains and wetlands trap particles, a process that is important for water quality and wetland function and morphology. The rates of particle removal by vegetation remain poorly characterized, especially for small particles and vegetation coated with biofilm. In this study, we measured capture rates of road dust by arrays of grass-like synthetic vegetation in a laboratory flume. We performed 40 experiments in which stem density, flow velocity, the presence of biofilm, and initial particle concentration varied, and used an in situ particle size analyzer to measure the concentration of a continuous particle size distribution (1.25–250 μm diameter). We fit first-order decay models to the particle concentration measurements to determine particle capture rates and found that capture rates increased with particle size, stem density, and the presence of biofilm. Capture rates decreased with increasing flow velocity, which suggests that fast flows may resuspend particles from stems. We also calculated percent particle capture efficiencies and fit a new empirical model for capture efficiency to our results. We found that particle capture efficiency was highest for low stem density treatments and propose that stem density affects capture by altering turbulent kinetic energy.

1. Introduction

The fate and transport of particles in floodplains and wetlands are fundamental to wetland form and function, pollutant and nutrient transport, primary productivity, land surface elevation, and downstream water quality [e.g., *Larsen and Harvey*, 2010; *Hosokawa and Horie*, 1992; *Davies-Colley and Smith*, 2001; *Mudd et al.*, 2010; *Johnston*, 1991]. Wetland vegetation is central to these processes by altering flow hydrodynamics and intercepting particles. Vegetation traps particles by either enhancing settling or by providing surfaces for particle adhesion [e.g., *Stumpf*, 1983; *Leonard et al.*, 1995; *Huang et al.*, 2008; *Saiers et al.*, 2003; *Kadlec and Wallace*, 2008; *Elliott*, 2000]. While gravitational settling dominates trapping of medium to large particles in vegetated zones under typical flow conditions [e.g., *Leonard et al.*, 1995; *Mudd et al.*, 2010], many particles are too small to settle on the time scale of floodplain inundation, even with vegetation-induced changes to turbulence intensity. As a result, trapping by plant stems may dictate capture rates for fine particles [e.g., *Huang et al.*, 2008].

The capture of a particle on a stem requires both contact between particle and stem (i.e., interaction) and particle adherence to the stem (i.e., retention) [*Defina and Peruzzo*, 2012]. While interaction and retention are essential for capture, laboratory studies often use silicon grease to ensure complete retention and target the dynamics of particle-stem interactions [i.e., *Palmer et al.*, 2004; *Purich*, 2006; *Harvey et al.*, 1995]. *Palmer et al.* [2004] examined capture by a single grease-coated cylinder and found an empirical relation for particle capture efficiency that has been widely applied. Furthermore, both *Harvey et al.* [1995] and *Palmer et al.* [2004] found that capture of 125–300 μm particles by a branch or a single cylinder is negatively correlated with collector diameter. A third study that used grease to guarantee retention found that capture efficiency varied with stem density and was highest for an intermediate density array (2026 rods m^{-2}) [*Purich*, 2006].

While the argument has been made that silicon grease serves as a biofilm analog, particle retention rates and mechanisms persist as unknowns in particle capture dynamics. Previous studies have shown that the

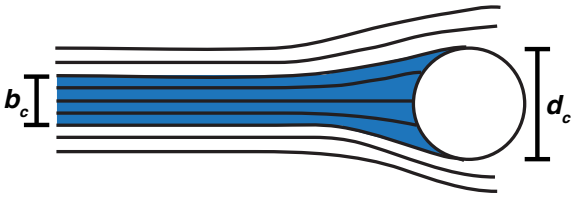

Figure 1. Particle capture efficiency, $\eta = \frac{b_c}{d_c}$, where b_c is the upstream width of particles that encounter a collector of diameter d_c.

presence of biofilm, composites of microorganisms and organic material such as periphyton that adhere to surfaces, increases particle capture [*Battin et al.*, 2003; *DiCesare et al.*, 2012]. Yet natural biofilms may not guarantee absolute retention and the *Palmer et al.* [2004] model does not include a parameter that explains the how biofilm or retention affects particle capture.

To date, no laboratory studies have examined particle capture by arrays of noncylindrical vegetation, used natural biofilms, a continuous range of particle sizes or particles smaller than 125 μm diameter in nonlaminar flows. The purpose of this study was to improve our understanding of particulate capture by vegetation by testing the influence of flow velocity, stem density, particle size, initial particle concentration, and the presence of biofilms on particle capture. Here we chose to examine the trapping of fine particle road dust due to the profound water quality implications of road dust runoff and ability of road dust to adsorb metals [*Swift et al.*, 2006; *Sansalone and Buchberger*, 1997]. To accomplish this, we conducted a series of laboratory flume experiments with bladed (grass-like) synthetic vegetation, natural biofilm, and suspended road dust, composed of a range of particle sizes. By measuring changes in suspended particle concentration through time, we examined how the presence of synthetic vegetation, with varying treatments, affected particle capture rates.

2. Methods

2.1. Theoretical Considerations

A number of processes can remove particles from suspension and these include: gravitational settling, direct interception, inertial impaction, and diffusional deposition [*Rubenstein and Koehl*, 1977; *Spielman*, 1977]. Settling is the sedimentation of particles or complex aggregated particles due to gravity. Particles can also be removed through impact and adherence to collectors such as plant leaves or stems. Direct interception is the capture of particles traveling along streamlines by collectors. Inertial impaction occurs when particles have sufficient momentum to deviate from their streamlines and impact collectors. Finally, diffusional deposition is the adherence of particles to collectors due Brownian motion or turbulence.

Capture by a collector can be parameterized by particle capture efficiency, η. Particle capture efficiency is defined as $\eta = \frac{b_c}{d_c}$, where b_c is the span width of a flow in which upstream particles will encounter a collector of diameter d_c (Figure 1). Particle capture efficiency defines the extent to which particles encounter and interact with collectors. However, only a fraction of particles, p_r, that interact with collectors will be retained. We therefore define effective particle capture as,

$$\eta' = p_r \frac{b_c}{d_c}. \tag{1}$$

Effective particle capture efficiency defines the efficiency with which collectors remove particles from suspension.

There are analytical expressions that describe capture efficiency as a function of collector Reynolds number and the ratio of particle diameter to collector diameter for creeping and potential flow [*Langmuir et al.*, 1942; *Fuchs*, 1964]. However, in transitionally turbulent conditions ($Re_c = 1–10^3$) where inertia matters and that are relevant to natural floodplains, empirical expressions are needed to describe particle capture efficiency. *Palmer et al.* [2004] fitted a power law function of the form $\eta \sim Re_c^m R^n$ to observations of direct interception of 177–210 μm by a single grease-coated cylinder in a laboratory flume and found that,

$$\eta = 0.224 Re_c^{0.718} R^{2.08}, \tag{2}$$

where $Re_c = \frac{u d_c}{\nu}$, u is flow velocity, ν is kinematic viscosity, and $R = \frac{d_p}{d_c}$ is the ratio of particle diameter, $d_{p,}$ to collector diameter. Because equation (2) was fitted to data from experiments using a single cylinder, single particle size class, and grease coating, equation (2) may not reflect natural wetland conditions (i.e., multiple stems and biofilm). This is important because, by generating wakes, vegetation stems affect flow velocities

and turbulence intensities and thus the trajectory of suspended particles [*Nepf*, 1999]. Moreover, by increasing drag, vegetation can slow flow and enhance settling. In this study, we measured suspended particle concentration to determine effective particle capture efficiencies and compare our results to equation (2).

We can derive an expression for the removal of suspended particles, and hence particle capture efficiency, according to a method presented by *Palmer et al.* [2004]. Consider flow past emergent vegetation. The rate that particles approach a stem within the region defined by the stem's frontal area is, $\overline{\phi} u d_c h_c$, when flow is steady, uniform, and unidirectional and where $\bar{\phi} = \frac{1}{h}\int_0^h \phi(z)dz$ is depth-averaged particle concentration, u is flow velocity, h_c is the stem length exposed to water, and h is water depth. From this flux, the number of particles captured by one collector over time, t, is $N_c = \eta' \bar{\phi} u d_c h_c t$. Furthermore, the number of suspended particles in a representative water volume, V, and with initial depth-averaged particle concentration, $\bar{\phi}_{t_1}$, due to capture by one collector is, $N(t) = \overline{\phi}_{t_1} V - \eta' u d_c h_c t$, and the rate of change of suspended particles is, $\frac{dN}{dt} = -\eta' u d_c h_c$

In a wetland with multiple stems $l_c = \frac{h_c}{V}$, where l_c is stem density and where h_c can have contributions from multiple stems. We can thus write a volumetric expression for the change in suspended particle concentration due to capture by multiple collectors as,

$$\frac{1}{V}\frac{dN}{dt} = \frac{-\eta' \bar{\phi} u d_c h_c}{V} = -\eta' \bar{\phi} u d_c l_c = \frac{d\bar{\phi}}{dt}. \tag{3}$$

Equation (3) shows how particle capture efficiency can be related to suspended particle concentration in a wetland or floodplain.

2.2. Suspended Particle Concentration Model

In this study, we measured the concentration of suspended particles (by size class) at a single point in a recirculating flume to quantify the removal of particles due to adherence to vegetation stems. Here we present our framework for evaluating the change in suspended particle concentration through time due to diffusion and gravitational settling. Consider a fully developed, steady, turbulent, unidirectional flow of depth h, where the x direction is along the flow, the y direction is cross stream to the flow, and the z direction is perpendicular to the flow. We also assume that particle concentration gradients are larger in the vertical direction than the downstream or cross-stream directions such that the evolution of suspended particle concentration for a specific particle size class can be described by an advection-diffusion equation of the form,

$$\frac{\partial \phi}{\partial t} = \frac{\partial}{\partial z}\left(D_z \frac{\partial \phi}{\partial z}\right) + v_s \frac{\partial \phi}{\partial z}, \tag{4}$$

where $\phi(z,t)$ is the concentration of particles in a specific size class, D_z(z) is the vertical diffusion coefficient, and v_s is the particle settling velocity. By integrating in the vertical direction from a location near the bed, b, to the top of the water column, h, specifying that there is vanishing normal upward sediment flux near the water surface (i.e., $\left(D_z \frac{\partial \phi}{\partial z} + v_s \phi\right)\Big|_h = 0$), dividing by h, and assuming $b \sim 0$ such that $\bar{\phi} \sim \frac{1}{h}\int_b^h \phi(z)dz$,

$$\frac{\partial \overline{\phi}}{\partial t} = -\frac{D_z|_b}{h}\frac{\partial \phi}{\partial z}\Big|_b - \frac{v_s}{h}\phi_b, \tag{5}$$

where ϕ_b refers to particle concentration near the bed. The first term on the right side of equation (5) is the entrainment rate of particles from the bed.

The Rouse equation approximates the vertical distribution of suspended sediment and is derived by balancing upward diffusion and downward sedimentation: $\phi(z) = \phi_a\left[\left(\frac{h-z}{z}\right)\left(\frac{a}{h-a}\right)\right]^{Z_R}$, where $\phi(z)$ is the concentration of particles at height z, ϕ_a is a reference concentration of particles at reference height a, and $Z_R = \frac{v_s}{\kappa u_*}$ is the Rouse number, $\kappa = 0.41$ is the Von Kármán constant and u_* is shear velocity [*Rouse*, 1950]. By differentiating the Rouse equation and evaluating the expression near the bed, $\frac{\partial \phi}{\partial z}|_b = -Z_R \phi_b \frac{h}{b(h-b)}$. Thus, equation (5) can be written as,

$$\frac{\partial \overline{\phi}}{\partial t} = -\frac{v_s}{h}(1 - E_r)\phi_b, \tag{6}$$

where $E_r = \frac{D_z|_b}{\kappa u_*}\frac{h}{b(h-b)}$ is a dimensionless entrainment rate of particles from the bed. Furthermore, by integrating the Rouse equation, dividing by h, and again assuming that $b \sim 0$ such that $\bar{\phi} \sim \frac{1}{h}\int_b^h \phi(z)dz$,

$$\bar{\phi} = \frac{1}{h}\int_b^h \phi(z)dz = \frac{\phi_a}{h}\int_b^h \left[\left(\frac{h-z}{z}\right)\left(\frac{a}{h-a}\right)\right]^{Z_R} dz = \frac{\phi_a}{C}. \quad (7)$$

Equation (7) shows how depth-averaged concentration can be related to concentration at a specific height with constant C that reflects the shape of the Rouse profile. By setting $a = b$, $\bar{\phi}$ can be related to ϕ_b and equation (6) becomes,

$$\frac{d\bar{\phi}}{dt} = -\frac{Cv_s}{h}(1-E_r)\bar{\phi}. \quad (8)$$

Now consider particle removal due to capture onto collectors, settling, and diffusion. By combining equations (3) and (8),

$$\frac{d\bar{\phi}}{dt} = -\left[\frac{Cv_s}{h}(1-E_r) + \eta' u d_c l_c\right]\bar{\phi} = -k\bar{\phi}, \quad (9)$$

where $k_s = \frac{Cv_s}{h}(1-E_r)$ is a particle removal rate due to settling, $k_c = \eta' u d_c l_c$ is a particle removal rate due to capture by plant stems, and k is the total particle capture rate. Note that k_s is negative when $E_r > 1$ (i.e., $D_z > \kappa u_* b$). Equation (9) can be integrated to find, $\bar{\phi}(t) = \bar{\phi}_o \exp(-kt)$, where $\bar{\phi}_o$ is initial depth-averaged particle concentration. Equation (9) shows that by measuring $\bar{\phi}(t)$ we can determine k. Furthermore, by substituting $\bar{\phi} = \frac{\phi_a}{C}$ from equation (7) into equation (9),

$$\phi_a(t) = \phi_{a_o}\exp(-kt). \quad (10)$$

Equation (10) shows that k can be determined by measuring $\phi(t)$ at a single depth in the water column (this study measured particle concentration 6.7 cm above the bed). In this study, we asses capture rate values by fitting equation (10) to measurements of suspended particle concentration and observe how changing experimental treatments affects particle capture rate, k.

2.3. Experimental Methods

This study used laboratory flume experiments to investigate the capture of suspended road dust particles by an array of synthetic vegetative stems. In brief, suspended road dust was recirculated through synthetic vegetation while particle concentration and size distribution were measured. Particle capture coefficients were fit (by size class) to measurements of particle concentration according to equation (10).

Specifically, a water volume of 0.75 m^3 was recirculated through a flume (7.90 m long $\times$ 0.46 m deep $\times$ 0.50 m wide) at three flow rates (1.2×10^{-3}, 3.2×10^{-3}, and 4.6×10^{-3} $m^3 s^{-1}$) (Figure 2). Each experiment ran for 63 min such that the water volume passed through the flume 6.2, 16.5, and 23.7 times for each respective flow rate (Table 2).

Suspended particle (road dust) volume concentration was measured with an in situ particle size analyzer (Sequoia LISST-100X; type B, size range 1.25–250 μm) (Figure 2). The LISST measures particle size distribution and concentration in 32 different size bins by laser diffraction techniques. Measurements from a given bin size were discarded if initial particle concentration was below 0.0005 μL L^{-1}, because the LISST does not reliably detect particles below that threshold (<10 data points discarded total). The LISST raw scattering intensities were processed using MATLAB© routines and assuming a refractive index of 1.17 [*Andrews et al.*, 2010]. These processing techniques have been shown to match road dust particle size distributions produced by microscopy [*Andrews et al.*, 2010]. The LISST was positioned on its side to prevent lens fouling, and measurements were made in the real-time burst-operating mode and reported at 1–9 s (average of 6 s) intervals. Experimental parameters were set to match naturally occurring values found in wetlands (Table 2).

Road dust particles were used because of their water quality implications. For example, highway runoff and urban storm water have been linked to a decline in Lake Tahoe clarity [*Swift et al.*, 2006]. The road dust used in this study was collected from the Lake Tahoe basin by a TYMCO DST-6 regenerative air sweeper in the Gardner Mountain subdivision, South Lake Tahoe, California, and is characterized by volcanic cinders, eroding sediment, and road material (R. Wigart, personal communication, 2012). It may also contain residues of traction sand that is applied to roadways during winter. A magnified image of the suspended road

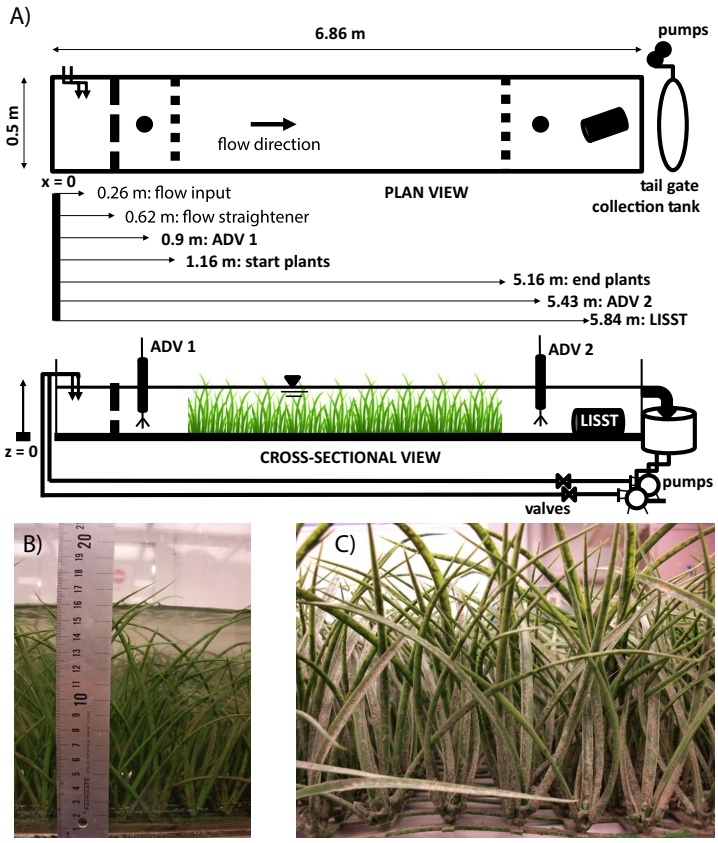

Figure 2. (a) Schematic of the flume experimental setup. Both plan and cross-sectional views are shown, (b) 2724 stems m^{-2} synthetic plants in the flume during an experiment, and (c) synthetic plants (green) coated with biofilm (brown) before an experiment.

dust particles demonstrates that the particles are nonspherical (supporting information Figure S1). While the road dust particles used in this study are nonspherical, the *Andrews et al.* [2010] processing routines have been shown to bin similar particles appropriately, according to mean diameter.

Road dust was suspended in tap water (conductance = 1146 ± 64 μS) at two starting particle concentrations (SPCs), 16.6 ± 6.5 μL L^{-1} (low SPC) and 28.4 ± 5.8 μL L^{-1} (high SPC). The high SPC initial particle size distribution (PSD) shows two modes of high concentration particles at 4 and 11 μm (Figure 3). The concentration maximum of 11 μm particles is due to filtering of the road dust during collection by a street sweeper.

To set the desired SPC value, particles were mixed in the flume until LISST transmission reached 75% or 55%, respectively. These transmission values were selected because they are within the LISST's optimal transmission range. To obtain the target SPC, road dust was stirred into the reservoir and then the pumps and LISST were turned on for 10–20 minutes to ensure thorough mixing of particles in the water reservoir and to monitor transmission values. During this time, additional particles were added to reach the desired transmission. After the target SPC was achieved, the pumps and LISST were turned off and the flume water drained into the reservoir for several minutes before an experiment was initiated.

While an experiment was running, water in the reservoir was agitated with the pumps as well as return water from the flume. Although it is possible that particle settling occurred in the reservoir during experimental runs, reservoir settling is independent of experimental treatment. Control runs can therefore be used to correct for reservoir settling (section 4). To avoid initialization effects, time zero for data analysis was set at 5 minutes after the LISST was turned on. Between experimental runs, water in the flume drained into the reservoir. Water and suspended particles were reused between experimental runs, but replaced approximately every six runs.

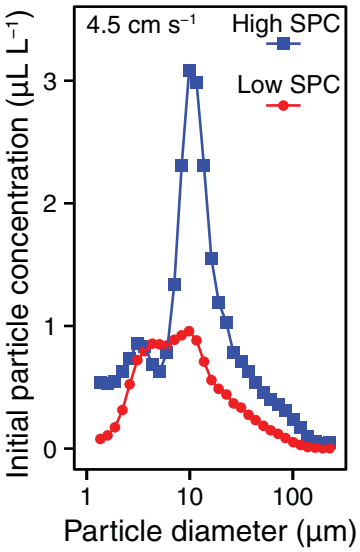

Figure 3. Initial particle size distributions of high and low starting particle concentration (SPC) experiments. These initial particle concentration values were averaged by velocity treatment and particle diameter. The high SPC initial particle size distribution shows two modes for 4 and 11 µm particles. By comparison, the initial particle size distribution of low SPC runs exhibits a single concentration maximum for 11 µm particles.

Plastic grass mats (0.46 m wide × 4.0 m long) with stem densities of 2724 and 7209 stems m^{-2} were used as the vegetation analog (Tables 1 and 2 and Figure 2). The mats consisted of bladed stems that were 6 mm wide by 1 mm thick at their base and 1 mm wide by 1 mm thick at their tips, and with average dimensions of 3 × 1 mm. The bladed stems were naturally bent and varied in length between 13.0 and 20.3 cm with average lengths of 14.5 cm (7209 stems m^{-2}) and 16.6 cm (2724 stems m^{-2}) (Figure 2). The stems did not visibly bend in response to the flow. The mats filled the entire width of the flume and, due to their buoyancy, were held to the flume with thin aluminum rods.

Biofilms were grown on the plastic mats to make the artificial grass more analogous to natural vegetation (Figure 2c). The plastic mats were submerged in Lake Spafford, a hypereutrophic body of water located on the UC Davis campus. After 1 week, the mats were extracted and gently rinsed to remove loosely attached organic material. The mats were dried outside for several days to simulate the natural conditions of intermittent floodplains that experience periods of extreme drought before flooding. Biofilm mass from a total of 56 stems was measured as 1.19×10^{-2} g biofilm per stem or 8.26×10^{-4} g cm^{-2}.

Flow velocities were measured using two methods. First, two 3D Acoustic Doppler Velocimeters (ADVs, Son-Tek) measured flow at 5 Hz in front of and behind the grass mats (Figure 2). Second, flow depths at the ADV locations were measured and used to calculate cross-sectional mean velocity. Flow rates were calibrated prior to experimental runs using a sluice gate and the three flow rate settings correlated with cross-sectional mean velocities with ranges of: 1.6–2.1, 4.0–5.0, and 5.8–6.8 cm s^{-1}; mean velocities of: 1.8, 4.5, and 6.1 cm s^{-1}, respectively. Four perforated aluminum screens (hole diameter 0.6 cm; 17,500 holes m^{-2}) were placed inside the flume upstream of the experimental vegetation to straighten the flow (Figure 2a).

Water surface slope measurements and vegetation density characteristics were used to calculate reach-averaged bed shear stress and shear velocities according to $\tau = \rho g S R_h - \frac{1}{2}\rho C_D l_c d_c h u^2$, where τ is bed shear stress, R_h is the hydraulic radius, ρ is water density, g is gravitational acceleration, S is water surface slope, and $C_D \sim 1$ is the drag coefficient for stiff cylinder-like vegetation [*Luhar and Nepf*, 2013]. We calculated reach-averaged shear velocities according to $u_* = \sqrt{\frac{\tau}{\rho}}$ and found u_* values of 5.53 ± 0.21 and 3.91 ± 1.06 cm s^{-1} for 0 and 2724 stems m^{-2} experiments, respectively. We use Stokes' law to calculate settling velocities and report Rouse numbers of 0.06 and 0.08 for 25 µm particles, 0.24 and 0.33 for 50 µm particles, 0.54 and 0.75 for 75 µm particles, and 0.96 and 1.33 for 100 µm particles and for 0 and 2724 stems m^{-2} treatments, respectively.

2.4. Particle Capture Mechanisms

Vegetation may have captured particles during these experiments through direct interception, diffusional deposition, and enhanced gravitational settling because vegetation can slow flow and reduce the shear velocities. We neglect inertial impaction because the Stokes number, which describes the influence of a particle's inertia, was ranged from 5×10^{-6} to 1.5×10^{-1} and was mostly below the critical value of 0.125 during this study [*Fuchs*, 1964].

2.5. Statistical Analysis

The influence of biofilm, initial particle concentration, flow velocity, and stem density on capture rates, k, was evaluated using analysis of variance (ANOVA) tests that determine whether the means of groups of data are equal by comparing the distributions of variances among groups. ANOVAs test the influence of fixed factors (differing experimental treatments such as biofilm or stem density) on the response variable

Table 1. Experimental Treatments

Run ID	Treatment	Flow Rate ($m^3\ s^{-1}$)	Velocity ($cm\ s^{-1}$)	Water Height (cm)	Starting Particle Concentration ($\mu L\ L^{-1}$)	SPC Standard Deviation
6a	7209 stems m^{-2}	0.0046	6.0	17.1	23.12	0.78
6b	7209 stems m^{-2}	0.0046	-	-	14.69	0.41
6c	7209 stems m^{-2}	0.0046	6.0	16.8	11.57	0.26
7a	7209 stems m^{-2} with biofilm	0.0012	1.8	14.7	13.50	0.78
7b	7209 stems m^{-2} with biofilm	0.0012	1.8	14.7	10.42	0.31
7c	7209 stems m^{-2} with biofilm	0.0012	1.8	14.7	11.09	0.23
8a	7209 stems m^{-2} with biofilm	0.0032	4.4	15.9	15.59	0.69
8b	7209 stems m^{-2} with biofilm	0.0032	4.4	15.8	9.61	0.14
8c	7209 stems m^{-2} with biofilm	0.0032	4.4	15.9	11.93	0.47
9a	7209 stems m^{-2} with biofilm	0.0046	5.9	17.0	16.49	0.67
9b	7209 stems m^{-2} with biofilm	0.0046	5.9	17.1	10.20	0.41
9c	7209 stems m^{-2} with biofilm	0.0046	5.9	17.0	9.57	0.27
10a	No plants (control)	0.0012	1.9	14.2	48.59	2.16
10b	No plants (control)	0.0012	1.9	14.2	33.64	1.47
11a	No plants (control)	0.0032	4.7	14.9	38.12	1.61
11b	No plants (control)	0.0032	4.7	14.8	29.08	1.29
12a	No plants (control)	0.0046	6.2	16.3	30.85	0.72
12b	No plants (control)	0.0046	6.2	16.3	26.28	0.89
13a	7209 stems m^{-2}	0.0012	1.8	14.5	32.21	0.80
13b	7209 stems m^{-2}	0.0012	1.8	14.5	25.51	0.54
14a	7209 stems m^{-2}	0.0032	4.6	15.3	28.24	0.82
14b	7209 stems m^{-2}	0.0032	4.6	15.3	25.40	0.95
15a	7209 stems m^{-2}	0.0046	6.0	16.7	25.73	0.69
15b	7209 stems m^{-2}	0.0046	6.0	16.7	22.94	0.52
16a	7209 stems m^{-2} with biofilm	0.0012	1.9	14.0	28.41	0.83
16b	7209 stems m^{-2} with biofilm	0.0012	1.8	14.3	24.05	0.54
17a	7209 stems m^{-2} with biofilm	0.0032	4.7	15.0	25.44	0.63
17b	7209 stems m^{-2} with biofilm	0.0032	4.7	15.1	26.41	0.74
18a	7209 stems m^{-2} with biofilm	0.0046	6.0	16.7	24.10	0.31
18b	7209 stems m^{-2} with biofilm	0.0046	6.0	16.7	25.31	0.44
19a	2724 stems m^{-2}	0.0012	1.7	15.3	18.45	0.52
19b	2724 stems m^{-2}	0.0012	-	-	16.66	0.57
20a	2724 stems m^{-2}	0.0032	4.6	15.2	18.69	0.50
20b	2724 stems m^{-2}	0.0032	4.6	15.3	11.50	0.69
21a	2724 stems m^{-2}	0.0046	6.1	16.6	13.15	0.56
21b	2724 stems m^{-2}	0.0046	-	-	24.60	1.07
22a	2724 stems m^{-2}	0.0012	1.9	13.9	32.61	1.25
22b	2724 stems m^{-2}	0.0012	1.9	13.5	24.87	0.53
23a	2724 stems m^{-2}	0.0032	4.8	14.8	25.15	0.73
23b	2724 stems m^{-2}	0.0032	4.8	14.6	22.14	0.65

(particle capture rate, *k*, for this study). To test all the factors in our experiment, different subsets of the data were used to perform the various ANOVAs. Within subsets, ANOVAs were compared with a type III sum of squares to determine the model with the best fit. Factors included stem density, particle diameter, biofilm, initial particle concentration, and flow velocity.

3. Results

In this study, we examined the impact of different stem densities, flow rates, presence of biofilm, and starting particle concentrations on particle capture rate, *k*, using an experimental flume setup. To calculate *k*, we fit first-order decay models to particle concentration measurements according to equation (10) (Figure 4).

Table 2. Experimental and Natural Floodplain Conditions

Parameter	Flume Experiments	Natural Floodplain	Reference
Channel average flow velocity ($cm\ s^{-1}$)	1.8; 4.5; 6.1	0–25	For example, *Valiela et al.* [1978]
Flow depth (cm)	14–17	0–50	*Kadlec* [1990]
Stem width (cm)	0.1–0.6	0.1–1.0	*Nepf* [2012]
Stem thickness (cm)	0.1	~0.1	*Nepf* [2012]
Stem (collector) Reynolds number	54–183	5–1000	*Kadlec* [1990]
Suspended particle concentration ($\mu L\ L^{-1}$)	9–50	9–25	For example, *Aiona* [2013]
Vegetation density (stems m^{-2})	0; 2724; 7209	0–2500	For example, *Valiela et al.* [1978]

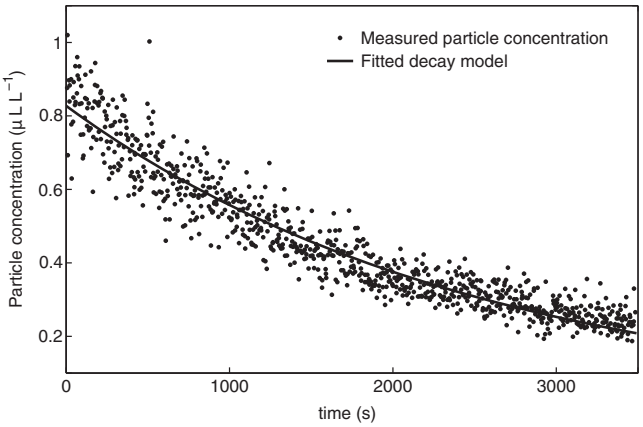

Figure 4. Time versus suspended particle concentration for a representative experiment (run 11a, 61.2 μm particles). The raw LISST measurements are shown with data points and the solid line is the model fit (equation (10)). The R^2 value for this fit is 0.91 and the capture rate, *k*, for this run is 3.95×10^{-4} s^{-1}

Higher values of *k* indicate greater particle capture. Equation (10) provides a good fit for the majority of particle sizes in this study (supporting information Figure S2). For most treatments, *k* increased with particle size, which agrees with predictions by equations (2, 8, and 9) (Figure 5). Equation (8) predicts that capture rates will increase with particle size because large particles settle faster and alter the shape of concentration profiles. Equations (2) and (9) also predict that both capture efficiency and rate increase with particle size [*Palmer et al.*, 2004].

Purich [2006] showed that stem density affected particle capture. However, stem density is not incorporated into current models for particle capture efficiency. To better understand how stem density relates to particle capture, we examined the impact of three stem density treatments, 0, 2724, and 7209 stems m^{-2}, on particle capture rate. Experimental runs including stems exhibited significantly higher removal rates compared to control runs without stems (Figures 5 and 6, supporting information Tables S1 and S3). This observation matched our

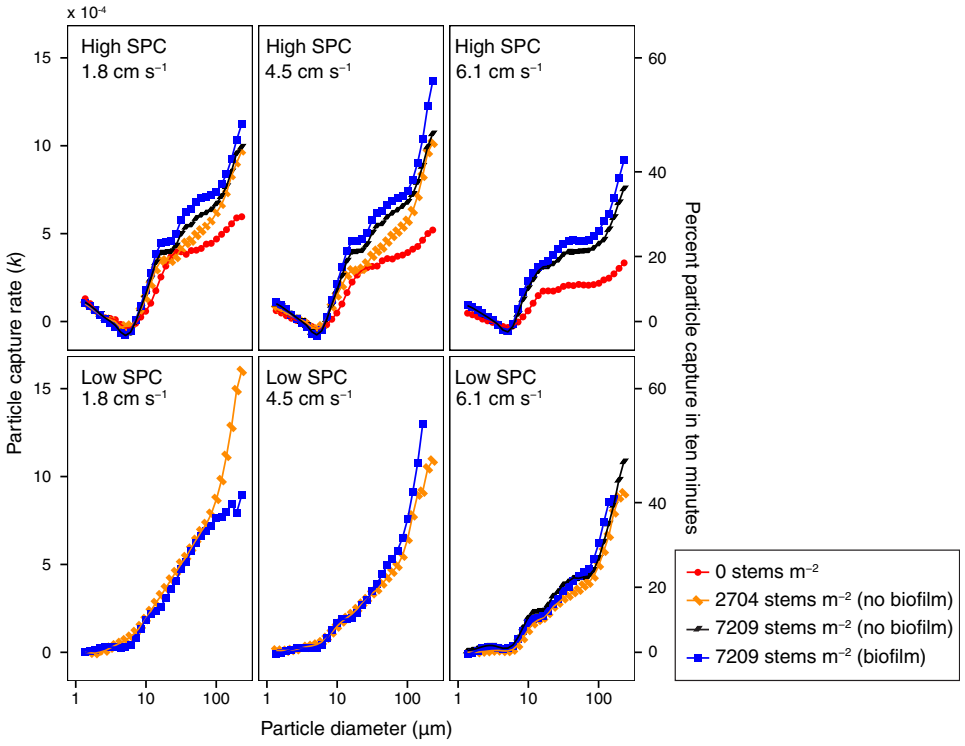

Figure 5. Particle capture rates and percent removal in 10 min plotted according to particle size for each experimental treatment. Treatments with biofilm demonstrate the highest capture rates followed by high stem density treatments. Control runs (0 stems m^{-2}) show the lowest capture rates. Capture rates from replicate runs (i.e., runs 8a–8c) were averaged to determine a single capture rate value for each treatment and particle diameter.

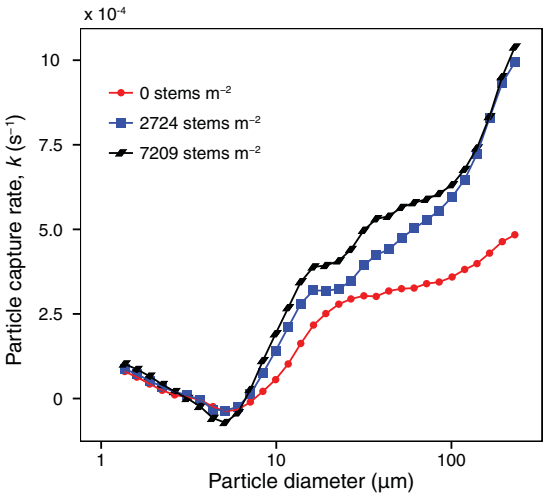

Figure 6. Particle diameters versus capture rate for differing stem density treatments: 0 stems m^{-2}, 2704 stems m^{-2}, and 7209 stems m^{-2}. High stem density treatments exhibit the highest capture rates for particles larger than 9 μm. Runs without vegetation exhibit the lowest capture rates. High SPC treatments without biofilm were averaged according to flow velocity to determine the plotted capture rates.

expectation that the presence of vegetation would aid in particle removal. Additionally, the higher-density treatment, 7209 stems m^{-2}, resulted in greater capture compared to the lower stem density treatment, 2724 stems m^{-2}, for most particle sizes (Figures 5 and 6).

Equation (2) predicts that capture efficiency increases with flow velocity. However, equation (2) is an empirical fit to experiments that used silicon grease to ensure complete retention [*Palmer et al.*, 2004]. In this study, we measured particle capture rates at three depth-averaged flow velocities (1.8, 4.5, and 6.1 cm s^{-1}) with biofilm-coated and plain stems. We found that flow velocity significantly affected capture rate (supporting information Tables S2–S4). Unlike equation (2), we found that capture rate declined with increasing flow velocity for most particle sizes and stem densities (Figures 5 and 7).

The composition of vegetation in natural wetland ecosystems is often diverse, and submerged stems are frequently covered in biofilm, which may alter the retention of particles that contact stems. To analyze the impact of biofilm on particle capture, we included stems covered in real biofilm as a treatment variable. We found that the rate of particle capture increased in the presence of biofilm for particles larger than approximately 10 μm (Figure 5 and supporting information Table S4).

Natural wetlands have variable suspended particle concentrations. To test whether initial concentration of particles suspended in the flume had an impact on capture rate, we conducted experiments using high and low starting particle concentrations (SPC). We found no overall impact of SPC on particle capture (ANOVA Pval = 0.5) (supporting information Table S5). We did, however, notice an interesting trend in the high SPC treatment not found in the low SPC treatment. For the smallest particle sizes, capture rate decreased as particle size increased. In fact, for particles in the 4.0–6.6 μm range, k was negative, indicating an increase in particle concentration of that size (Figures 5–7). By comparison, the low SPC treatments demonstrated

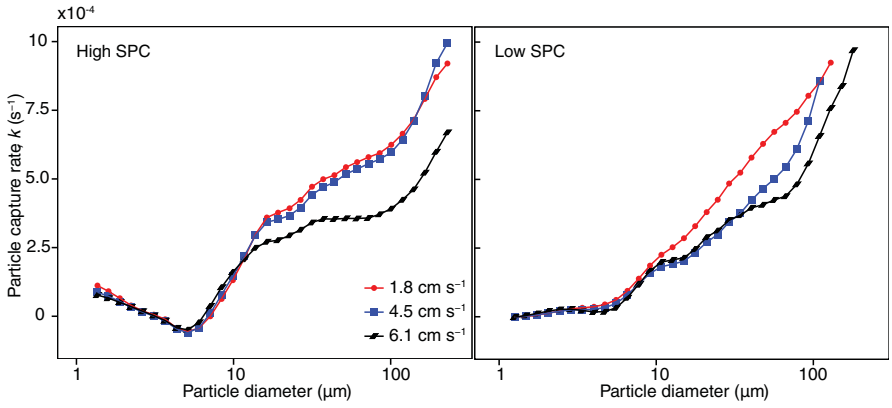

Figure 7. Particle diameters versus capture rate differing flow velocity treatments: 1.8, 4.5, and 6.1 cm s^{-1}. Capture rates are generally highest for 1.8 cm s^{-1} and lowest for 6.1 cm s^{-1} treatments. Capture rates for high SPC treatments without biofilm were averaged by particle size class and plotted on the left; averages for low SPC treatments are shown on the right. By comparison to high SPC runs, particle capture rates increase smoothly with particle size for low SPC runs. Otherwise, high and low SPC treatments exhibit similar capture rates.

positive removal rates for all particle size classes (Figures 5 and 7b). We suspect that flocculation of small particles in the high SPC treatment is responsible and discuss this possibility in supporting information section S2.

4. Scaling From Flume to Floodplain

Here we separate particle settling rate, k_s, from plant capture rates, k_c. We also apply a scaling parameter to k_c to correct for the intermittent exposure of water and suspended particles to plants during the experiments.

Equation (9) shows how the measured capture rate is the sum of capture due to settling and trapping by plant stems. Therefore, to determine k_c, we subtract k_s from k. We use control runs with no stems (high SPC runs) to estimate k_s, the removal rate of particles due to settling in the flume and reservoir. Because adding vegetation to the flume enhances settling compared to control runs by reducing shear velocities, we underestimate k_s for runs with vegetation [*Lopez and Garcia*, 1997].

We correct for the exposure of water to synthetic vegetation by multiplying the difference between k and k_s by the ratio of travel times through the flume versus plants in the flume. The time it takes the volume of water in the flume, V_T, to complete one cycle through the flume is $\frac{V_T}{uwh}$, where u is mean flow velocity and w is flume width. The travel time through the vegetated reach is $\frac{L}{u}$, where L is the length of the vegetated reach (Figure 2). The capture rate due to removal by vegetation stems is thus,

$$k_c = \frac{V_T}{Lwh}(k^i - k_s^i), \tag{11}$$

where i is the particle bin size, k^i is the measured capture rate from runs with vegetation, and k_s^i is a capture rate from control runs averaged by bin size for each experimental treatment. k_c values are useful because they reflect particle capture by vegetative stems, can be used to calculate particle capture efficiencies, and are independent of Rouse profile shapes.

5. Discussion

5.1. Particle Capture Efficiency

Many studies have used particle capture efficiency to characterize particle capture by a collector [e.g., *Spielman*, 1977; *Shimeta and Jumars*, 1991; *Palmer et al.*, 2004; *Purich*, 2006; *Wu et al.*, 2011] (Figure 1). We calculated effective particle capture efficiencies, η', from capture rates, k_c, using equations (3) and (9). We plot η' against Re_c (particle diameter = 101 μm and $R = 0.033$) and alongside η results from *Purich* [2006] (particle diameter = 230 μm and $R = 0.037$) and predictions by *Palmer et al.* [2004] (equation (8), $R = 0.033$) (Figure 8 and Table 3 and supporting information Table S6). In contrast to *Palmer et al.* [2004], we found that η' decreased with Re_c (Figure 8). *Purich* [2006] also found that η decreased with Re_c for intermediate density (2026 stems m^{-2}) arrays, but is unaffected by Re_c at other stem densities (Figure 8).

The differing relationships between capture efficiency and flow velocity observed among the different studies may result from differences in particle retention, the ability of particles to adhere to a collector after impact. The probability of particle capture, P_c, can be expressed as a function of particle retention and particle-stem interaction, $P_c = P_i \times P_r$, where P_i is the probability that a particle collides with a stem and P_r is the probability that a particle remains adhered to the stem after interaction [*Defina and Peruzzo*, 2010, 2012; *Peruzzo et al.*, 2012]. During the *Palmer et al.* [2004] and *Purich* [2006] studies, the probability of particle retention was 100% because cylinders were coated with grease (Table 3). By comparison, an unknown fraction of particles that impacted stems were retained during our experiments. In other words, *Palmer et al.* [2004] and *Purich* [2006] measured capture efficiency, η, while this study measured effective capture efficiency, η'.

For capillary trapping of floating particles by vegetation, *Peruzzo et al.* [2012] showed that capture probability decreased as drag force on the particle (a function of flow velocity) increased relative to the capillary forces holding particles to stems. During our experiments, a similar phenomenon may have occurred in which fewer particles were retained at higher flow velocities as drag forces on a particle increased relative to the adhesive forces holding particles to stems, effectively knocking particles off the stems. *Peruzzo et al.*

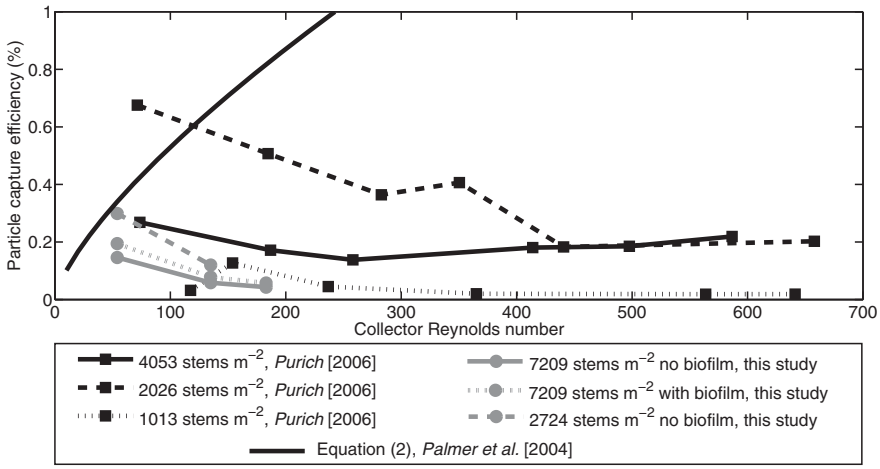

Figure 8. Effective capture efficiencies from this study (101 μm particles, $R = 0.033$), *Purich* [2006] (230 μm particles, $R = 0.037$), and predictions by *Palmer et al.* [2004] ($R = 0.033$). Measurements of effective capture efficiency by this study and *Purich* [2006] show a decrease in, or no relationship between, effective capture efficiency and Re_c. *Palmer et al.* [2004] predicts an increase in capture efficiency with Re_c.

[2012] demonstrated that this effect lowers particle retention, and therefore capture efficiency, as flow velocity increases. We propose that particle capture declined because particle retention declined as flow velocity increased during our experiments.

It is worth noting that *Purich* [2006] observed a flat to negative correlation between capture efficiency and flow velocity despite using grease to ensure complete particle retention. *Purich* [2006] attributed this difference to changes in the relative importance of turbulent/diffusional deposition and inertial impaction in their study versus *Palmer et al*. [2004].

We also found that effective capture efficiency varied with stem density. During our experiments, effective capture efficiencies were higher for the low, 2724 stems m^{-2}, treatments compared to the high, 7209 stems m^{-2}, treatments (Figure 8). This is in contrast to capture rates (s^{-1}), which were highest for the high stem density treatments. This is because capture rates integrate the effects from multiple stems and therefore increase with stem density for a given efficiency. Similar to our findings, *Purich* [2006] observed that 2026 stems m^{-2} treatments resulted in higher capture efficiencies compared to 4053 and 1013 stems m^{-2} treatments (Figure 8). Together, these findings suggest that capture efficiency is a function of stem density and therefore equation (2) should be modified to account for stem density.

In addition, *Purich* [2006] observed that flow velocity fluctuations were largest for this intermediate stem density treatment (reported through velocity standard deviations). *Purich* [2006] also found that a low stem density treatment (1013 stems m^{-2}) exhibited the second highest capture efficiencies and velocity fluctuations. Because turbulent kinetic energy (TKE) scales with turbulent velocity fluctuations, these observations suggest that capture efficiency increases with TKE. It is conceptually consistent for capture efficiency to increase with TKE because the number of particle-stem interactions increases with turbulent diffusion, which is proportional to TKE$^{1/2}$ [*Nepf*, 1999].

Table 3. Study Parameter Comparison

Study	Particle Diameter (μm)	Particle Type	Collector Diameter (cm)	Collector Type	Stem Density (stems m^{-2})	Flow Velocity (cm s^{-1})	Collector Reynolds Number (Re_c)	Particle Diameter: Collector Diameter
This study	1.25–250	Road dust	0.1–0.6 (0.3 average)	Bladed plastic stems (some with biofilm)	2724; 7209	1.8; 4.5; 6.1	54–183	0.0004–0.083
Purich [2006]	212–250	Pliolite particles	0.63	grease-coated cylinders	1013; 2026; 4053	1–10.2	70–640	0.037
Palmer et al. [2004]	177–210	Plastic resin	0.64; 1.27; 2.54	grease-coated Delrin® cylinder	Single cylinder	0.6; 1.1; 1.8	38–486	0.008; 0.016; 0.03

Furthermore, it has been shown that TKE reaches a maximum in intermediate density arrays (precise stem density determined by bed drag and vegetation height and geometry) given constant external forcing (i.e., water surface slope) [*Nepf*, 1999]. This is because vegetative stems generate turbulence but also add velocity-reducing drag [*Nepf*, 2012]. As a result, capture efficiencies may be highest for intermediate stem density arrays where TKE is maximized. Depth-averaged TKE can be calculated as a function of stem density, flow velocity, bed friction velocity, and bulk drag of the vegetative array [*Nepf*, 1999]. As a result, wetland engineers that wish to maximize capture efficiency may seek stem densities and geometries that maximize TKE.

5.2. New Relation for Particle Capture Efficiency

While the efficiency of particle impaction may be accurately described by the *Palmer et al.* [2004] model, the efficiency of particle capture in natural wetland ecosystems is better estimated by our experiments that used realistic stem surfaces. Thus, we fitted a new empirical expression for effective capture efficiency of the form $\eta' \sim Re_c^m R^n$ to our results. We used effective capture efficiencies calculated from high SPC, 7209 stems m^{-2} runs without biofilm ($Re_c = 54–183$, $R = 0.01–0.083$, $d_c = 3$ mm) and found that,

$$\eta' = 1.53 Re_c^{-1.14} R^{0.65}, \quad (R^2 = 0.87). \tag{12}$$

We compared this expression to other experimental treatments (high SPC, 7209 stems m^{-2} runs with biofilm and high SPC, 2724 stems m^{-2} runs without biofilm) and found that the exponents for Re_c ($m = -1.14$) and R ($n = 0.65$) match the trends in the data. To account for the effects of stem density and biofilm on capture, we adjusted the scalar coefficient in equation (12). We found that for 7209 stems m^{-2} with biofilm treatments,

$$\eta' = 2.06 Re_c^{-1.14} R^{0.65}, \quad (R^2 = 0.87). \tag{13}$$

For 2724 stems m^{-2} without biofilm,

$$\eta' = 3.18 Re_c^{-1.14} R^{0.65}, \quad (R^2 = 0.82). \tag{14}$$

This study's effective particle capture efficiencies better correlate with predicted efficiencies from equations (12–14) than those calculated using equation (2) from *Palmer et al.*, [2004] (Figure 9).

We found that effective capture efficiency scales such that $\eta' \sim \frac{\sqrt{R}}{Re_c}$ while *Palmer et al.* [2004] found that $\eta \sim Re_c^{3/4} R^2$. If our interpretation of particle retention is correct (section 5.1), the contrast between these capture efficiency relations implies that an increase in flow velocity resulted in twice as many particle resuspension events as particle-stem interaction events.

In this study, we found that particle capture increased with particle size, a trend that agrees with *Palmer et al.* [2004]. However, *Palmer et al.* [2004] predicted a larger increase in capture with particle size than we found (Figure 8). Lower retention of large particles may be responsible for this behavior because drag forces, which scale with velocity squared and particle frontal area, resuspend larger particles more easily than smaller particles.

5.3. Biofilm

The result that the presence of biofilm enhanced capture rates and efficiencies (Figures 8 and 9) motivates questions about how biofilm enhances particle retention or particle-stem interactions. Possible mechanisms for retention include stickiness [*Battin et al.*, 2003], roughness, and surface properties such as zeta potential. Colloid filtration studies have shown that the effectiveness of colloid interception by a collector depends on zeta potential (charge of the electrokinetic double layer) of the filter media/collector [e.g., *Yao et al.*, 1971]. *DiCesare et al.* [2012] found that oocyst retention on biofilm was strongly correlated with biofilm roughness. However, roughness elements also increase the probability of interaction between a particle and collector. *Palmer et al.* [2004] showed that adding roughness elements to a grease-cylinder increased particle capture efficiency when retention was 100%.

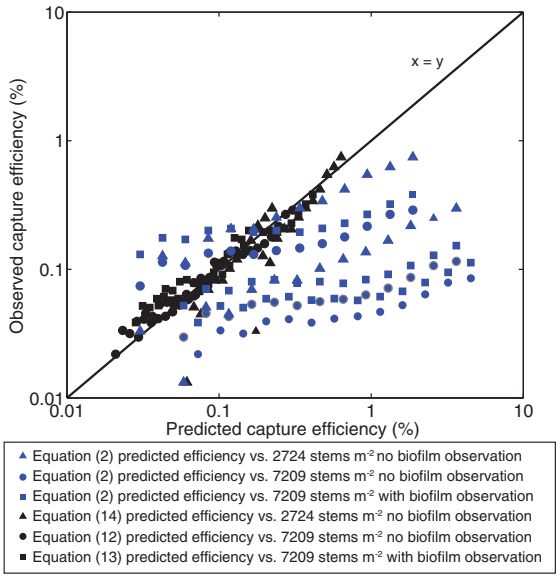

Figure 9. Effective capture efficiencies observed by this study ($Re_c = 54$, 135, and 183 and $R > 0.01$) plotted against predicted capture efficiencies. Predicted efficiencies are calculated from *Palmer et al*. [2004] (equation (2), $d_c = 3$ mm) and equations (12)–(14). Equations (12)–(14) were developed by fitting a power law function of the form $\eta \sim Re_c^m R^n$ to observations of effective capture efficiency, and match our experimental observations better than Equation (2).

Regardless of the mechanism through which biofilm affects particle capture, biofilms grow, decay, and become dormant. Thus, there is a temporal component to particle capture rates and efficiency due to a changing probability for particle retention. *Jin et al*. [2011] examined particle capture by fresh versus dried and then rehydrated biofilms on slides in a laboratory setting and found that rehydrated biofilms do not retain particles as effectively as fresh biofilms. We used dried and rehydrated biofilms in this study, and results from *Jin et al*. [2011] suggest that capture efficiency may be higher in natural environments with fresh biofilms.

6. Conclusions

This study examined particle capture by emergent, synthetic vegetation in a laboratory flume. The results are particularly important as they are derived from a natural, continuous particle distribution, that includes micron-scale particle sizes, 1.25–250 μm, and were conducted using vegetation-like arrays. By fitting first-order kinetics models to measurements of suspended concentration, we found that the presence of synthetic vegetation increased particle capture rates (s^{-1}) compared to a bare flume. Moreover, capture rates increased with particle size, stem density, and the presence of biofilm. The removal rate of fine particles, <30 μm, was lower than that of the larger particle fraction, yet removal was positive for particles larger than 10 μm. Particle capture rates did not change as a function of initial particle concentration.

We calculated effective particle capture efficiency (percent) and found that efficiency varied with stem density and was higher for the 2724 stems m^{-2} treatment compared to the 7209 stems m^{-2} treatment. *Purich* [2006] found that capture efficiency and TKE were highest for a 2026 stems m^{-2} treatment compared to 1013 and 4053 stems m^{-2} treatments. These results suggest that capture efficiency depends nonlinearly on stem density and is highest in intermediate density arrays where TKE is largest.

Contrary to equation (2), we find that effective capture efficiency and rate decrease with collector Reynolds number. While the number of particle-stem interaction events may increase with Re_c (due to an increase in turbulent diffusion), higher flow velocities have been shown to resuspend a greater portion of particles from stems [*Peruzzo et al*., 2012]. Because particle retention by stems was less than 100% in this study, we attribute the inverse relationship between capture and flow velocity to decreasing particle retention with increasing flow velocity. We fitted new empirical expressions for effective capture efficiency as a function of Re_c and R that reflect this negative correlation.

We observed that the presence of biofilm increased particle capture and suggest that biofilm increases the retention of particles by plant stems. However, more work is needed to determine how surfaces properties affect particle retention and to develop a mechanistic expression for capture efficiency as a function of particle-stem interactions and particle retention.

Our results provide a number of important lessons for floodplain management. First, our results suggest that artificial floodplains and restoration projects designed to optimize particle capture should strive for low flow velocities to minimize particle resuspension and maximize settling. While high stem density treatments captured more particles than low stem density treatments, capture efficiency was highest for the low stem density treatment. There may be marginal gains when increasing stem density past a value that maximizes

TKE. Finally, the positive impact of biofilms on capture suggests that surface properties affect particle retention and long-term capture. Because natural biofilms have growth cycles that likely affect surface properties, there is an additional time component inherent in the operation of floodplains and efficiency of particle capture.

Notation

η particle capture efficiency, dimensionless.
b_c upstream width of particles that are captured by a collector, m.
d_c collector (stem) diameter, m.
p_r fraction of particles retained by collectors, dimensionless.
η' effective particle capture efficiency, dimensionless.
Re_c collector Reynolds number, dimensionless.
u flow velocity, m s^{-1}.
ν kinematic viscosity, m^2 s^{-1}.
R particle diameter to stem diameter ratio, dimensionless.
d_p particle diameter, μm.
$\overline{\phi}$ depth-averaged particle concentration, μL L^{-1}.
h_c length of vegetation stems exposed to water, m.
h water depth, m.
N_c number of particles captured by a collector, number particles.
N number of particles in suspension, number particles.
t time, s.
V volume of water in a representative volume, m^3.
l_c stem density/collector length per unit volume, m m^{-3}.
ϕ particle concentration in a specific size class, μL L^{-1}.
D_z vertical diffusion coefficient, m^2 s^{-1}.
v_s particle settling velocity, m s^{-1}.
b location near the bed, m.
ϕ_b particle concentration near the bed, μL L^{-1}.
a reference height above the bed, m.
ϕ_a particle concentration at reference height a, μL L^{-1}.
Z_R Rouse number, dimensionless.
κ Von Kármán constant, dimensionless.
u_* shear velocity, m s^{-1}.
E_r entrainment flux, dimensionless.
C constant that reflects shape of Rouse profile, dimensionless.
k_s particle removal rate due to settling, s^{-1}.
k_c particle removal rate due to capture by plant stems, s^{-1}.
k total particle removal rate, s^{-2}.
$\overline{\phi}_o$ initial depth-averaged particle concentration, μL L^{-1}.
ϕ_{a_o} initial particle concentration at depth a, μL L^{-1}.
τ shear stress, kg m^{-1} s^{-2}.
g gravitational acceleration, m s^{-2}.
ρ water density, kg m^3.
C_D Drag coefficient, dimensionless.
R_h hydraulic radius, m.
S water surface slope, m m^{-1}.
St Stokes number, dimensionless.
V_T volume of water in circulation in the flume, m^3.
w width of flume, m.
L length of vegetated reach in the flume, m.
V_p volume of water in synthetic vegetation, m^3.
P_c probability of capture, percent.

P_i probability of particle-stem interaction, percent.
P_r probability of particle retention, percent.

Acknowledgments
This work was supported by a grant from the U.S. Department of Agriculture Forest Service Pacific Southwest Research Station using funds provided by the Bureau of Land Management through the sale of public lands as authorized by the Southern Nevada Public Lands Management Act (SNPLMA) under grant USFS 11-JV-11272170-092. The lead author was partly supported by a National Science Foundation Graduate Student Fellowship and a California Lake Management Society Scholarship. We gratefully acknowledge D. Kehlet and B. Sluis for their help modifying the flume, A. Luo for assistance running the experiments, and A. Bryk, K. Reardon and I. Rose for thoughtful discussions. We thank W. E. Fleenor for input to flume design and for providing the ADVs and thank R. Wigart for supplying and D. Hunter for imaging the road dust particles. Thoughtful review by M. Manga and J. E. Reuter, Water Resources Research Editors Anna M. Michalak and Francesco Comiti, and two anonymous reviewers greatly improved this manuscript. Please go to http://seismo.berkeley.edu/~kfauria/ParticleCapture-DataRepository.zip to access the raw data in this paper.

References

Aiona, A. (2013), Can a constructed stormwater facility remove fine particles from urban runoff?, MS thesis, Dep. of Civ. and Environ. Eng., Univ. of Calif., Davis, Davis.
Andrews, S., D. Nover, and S. Schladow (2010), Using laser diffraction data to obtain accurate particle size distributions: The role of particle composition, *Limnol. Oceanogr. Methods*, *8*, 507–526, doi:10.4319/lom.2010.8.507.
Battin, T. J., L. A. Kaplan, J. D. Newbold, and C. M. Hansen (2003), Contributions of microbial biofilms to ecosystem processes in stream mesocosms, *Nature*, *426*(6965), 439–442, doi:10.1038/nature02152.
Davies-Colley, R., and D. Smith (2001), Turbidity, suspended sediment, and water clarity: A Review, *J. Am. Water Resour. Assoc.*, *37*, 1085–1101.
Defina, A., and P. Peruzzo (2010), Floating particle trapping and diffusion in vegetated open channel flow, *Water Resour. Res.*, *46*, W11525, doi:10.1029/2010WR009353.
Defina, A., and P. Peruzzo (2012), Diffusion of floating particles in flow through emergent vegetation: Further experimental investigation, *Water Resour. Res.*, *48*, W03501, doi:10.1029/2011WR011147.
DiCesare, E. W., B. R. Hargreaves, and K. L. Jellison (2012), Biofilm roughness determines *Cryptosporidium parvum* retention in environmental biofilms, *Appl. Environ. Microbiol.*, *78*(12), 4187–4193, doi:10.1128/AEM.08026-11.
Elliott, A. (2000), Settling of fine sediment in a channel with emergent vegetation, *J. Hydraul. Eng.*, *126*, 570–577, doi:10.1061/(ASCE)0733-9429(2000)126:8(570).
Fuchs, N. A. (1964), *The Mechanics of Aerosols*, edited by R. E. Daisley and M. Fuchs, Pergamon, N. Y.
Harvey, M., E. Bourget, and R. G. Ingram (1995), Experimental evidence of passive accumulation of marine bivalve larvae on filamentous epibenthic structures, *Limnol. Oceanogr.*, *40*, 94–104.
Hosokawa, Y., and T. Horie (1992), Flow and particulate nutrient removal by wetlands with emergent macrophytes, in *Marine Coastal Eutrophication: Science of the Total Environment*, edited by R. Vollenweider, R. Marchetti, and R. Viviani, pp. 1271–1282, Amsterdam, Elsevier Pub., Colo.
Huang, Y. H., J. E. Saiers, J. W. Harvey, G. B. Noe, and S. Mylon (2008), Advection, dispersion, and filtration of fine particles within emergent vegetation of the Florida Everglades, *Water Resour. Res.*, *44*, W04408, doi:10.1029/2007WR006290.
Jin, Y., A. Aiona, S. G. Schladow, and S. Wuertz (2011), Biofilms in floodplain retain inorganic fine particles present in stormwater, paper presented at IWA Biofilm Conference 2011: Processes in Biofilms, Tongjji Univ., Shanghai, China, 27–30 Oct.
Johnston, C. A. (1991), Sediment and nutrient retention by freshwater wetlands: Effects on surface water quality, *Crit. Rev. Environ. Control*, *21*, 491–565.
Kadlec, R. (1990), Overland Flow in Wetlands: Vegetation Resistance, *J. Hydraul. Eng.*, *116*(5), 691–706.
Kadlec, R. H., and S. Wallace (2008), *Treatment Wetlands*, CRC Press, Boca Raton, Fla.
Langmuir, I., W. H. Rodebush, and V. K. Lamer (1942), Filtration of aerosols and development of filter materials, *Rep. OSRD-865*, Off. of Sci. Res. and Dev., Washington, D. C.
Larsen, L. G., and J. W. Harvey (2010), How vegetation and sediment transport feedbacks drive landscape change in the Everglades and wetlands worldwide, *Am. Nat.*, *176*, E66–E79, doi:10.1086/655215.
Leonard, L. A., A. C. Hine, and M. E. Luther (1995), Surficial sediment transport and deposition processes in a Juncus roemerianus marsh, west-central Florida, *J. Coastal Res.*, *11*, 322–336.
Lopez, F., and M. Garcia (1997), Open-channel flow through simulated vegetation: Turbulence modeling and sediment transport, *Tech. Rep. WRP-CP-10*, Waterw. Exp. Stn., U.S. Army Corps of Eng., Vicksburg, Miss.
Luhar, M., and H. M. Nepf (2013), From the blade scale to the reach scale: A characterization of aquatic vegetative drag, *Adv. Water Res.*, *51*, 305–316, doi:10.1016/j.advwatres.2012.02.002.
Mudd, S. M., A. D'Alpaos, and J. T. Morris (2010), How does vegetation affect sedimentation on tidal marshes? Investigating particle capture and hydrodynamic controls on biologically mediated sedimentation, *J. Geophys. Res.*, *115*, F03029, doi:10.1029/2009JF001566.
Nepf, H. M. (1999), Drag, turbulence, and diffusion in flow through emergent vegetation, *Water Resour. Res.*, *35*, 479–489, doi:10.1029/1998WR900069.
Nepf, H. M. (2012), Flow and transport in regions with aquatic vegetation, *Annu. Rev. Fluid Mech.*, *44*, 123–142, doi:10.1146/annurev-fluid-120710-101048.
Palmer, M. R., H. M. Nepf, T. J. Pettersson, and J. D. Ackerman (2004), Observations of particle capture on a cylindrical collector: Implications for particle accumulation and removal in aquatic systems, *Limnol. Oceanogr. Methods*, *49*, 76–85.
Peruzzo P., A. Defina, and H. Nepf (2012), Capillary trapping of buoyant particles within regions of emergent vegetation, *Water Resour. Res.*, *48*, W07512, doi:10.1029/2012WR011944.
Purich, A. (2006), The capture of suspended particles by aquatic vegetation, PhD thesis, Sch. of Environ. Syst. Eng., Univ. of West. Aust., Perth.
Rouse, H. (1950), *Engineering Hydraulics*, John Wiley, N. Y.
Rubenstein, D. I., and M. Koehl (1977), The mechanisms of filter feeding: Some theoretical considerations, *Am. Nat.*, *111*, 981–994.
Saiers, J. E., J. W. Harvey, and S. E. Mylon (2003), Surface-water transport of suspended matter through wetland vegetation of the Florida everglades, *Geophys. Res. Lett.*, *30*(19), 1987, doi:10.1029/2003GL018132.
Sansalone, J. J., and S. G. Buchberger (1997), Partitioning and first flush of metals in urban roadway storm water, *J. Environ. Eng.*, *123*(2), 134–143.
Shimeta, J., and P. A. Jumars (1991), Physical mechanisms and rates of particle capture by suspension feeders, *Oceanogr. Mar. Biol. Annu. Rev.*, *29*, 191–257.
Spielman, L. A. (1977), Particle capture from low-speed laminar flows, *Annu. Rev. Fluid Mech.*, *9*, 297–319.
Stumpf, R. P. (1983), The process of sedimentation on the surface of a salt marsh, *Estuarine Coastal Shelf Sci.*, *17*, 495–508.
Swift, T. J., J. Perez-Losada, S. G. Schladow, J. E. Reuter, A. D. Jassby, and C. R. Goldman (2006), Water clarity modeling in Lake Tahoe: Linking suspended matter characteristics to Secchi depth, *Aquat. Sci.*, *68*, 1–15, doi:10.1007/s00027-005-0798-x.
Valiela, I., J. M. Teal, and W. G. Deuser (1978), The nature of growth forms in the salt marsh grass Spartina alterniflora, *Am. Nat.*, *112*, 461–470.
Wu, L., B. Gao, and R. Munoz-Carpena (2011), Experimental analysis of colloid capture by a cylindrical collector in laminar overland flow, *Environ. Sci. Technol.*, *45*(18), 7777–7784, doi:10.1021/es201578n.
Yao, K., M. T. Habibian, and C. R. O'Melia (1971), Water and waste water filtration. Concepts and applications, *Environ. Sci. Technol.*, *5*, 1105–1112.